Necroptosis Triggered by ROS Accumulation and Ca2+ Overload, Partly Explains the Inflammatory Responses and Anti-Cancer Effects Associated With 1Hz, 100 mT ELF-MF *in vivo*

Mojdeh Barati
Breast Cancer Research Center, Motamed Cancer Institute, ACECR
Mohammad Amin Javidi
Breast Cancer Research Center, Motamed Cancer Institute, ACECR
Behrad Darvishi
Breast Cancer Research Center, Motamed Cancer Institute, ACECR
Seyed Peyman Shariatpanahi
university of Tehran
Zahra S. Mesbah Moosavi
York University Toronto, ON, canada
Reyhane Ghadirian
Breast Cancer Research Center, Motamed Cancer Institute, ACECR
Tahereh Khani
Breast Cancer Research Center, Motamed Cancer Institute, ACECR
Hassan Sanati
Breast Cancer Research Center, Motamed Cancer Institute, ACECR
Hossein Simaee
Breast Cancer Research Center, Motamed Cancer Institute, ACECR
Mahdieh Shokrollahi Barough
Breast Cancer Research Center, Motamed Cancer Institute, ACECR
Leila Farahmand
Breast Cancer Research Center, Motamed Cancer Institute, ACECR
Alireza Madjid Ansari (majidansari@acecr.ac.ir)
Breast Cancer Research Center, Motamed Cancer Institute, ACECR https://orcid.org/0000-0002-3043-7145

Research

Keywords: Necroptosis, extremely low frequency magnetic field, ROS, Calcium, RIPK1, RIPK3, MLKL

Posted Date: September 22nd, 2020

DOI: https://doi.org/10.21203/rs.3.rs-74744/v1

Version of Record: A version of this preprint was published at Free Radical Biology and Medicine on June 1st, 2021. See the published version at https://doi.org/10.1016/j.freeradbiomed.2021.04.002.

Abstract

Background: Focus on application of non-ionizing, extremely low frequency magnetic fields (ELF-EMF) as an alternative approach for treating cancer is rapidly rising nowadays. Nevertheless, little is known about the underlying anti-tumoral mechanism of action of them.

Methods: In the present study, for the first time, we reported that along with apoptosis, 2 h/day exposure to 100 Hz, 1 mT ELF-EMF for a 5-day period, can induce necroptosis, a specific type of programed necrotic cell death, by promoting RIPK1/RIPK3/MLKL pathway which may also be responsible for observed pro-inflammatory responses *in vivo*, evident from an increase in plasma levels of pro-inflammatory cytokines including TNF-α, IL-1β, IL-2, IL-6, IL-17A and IFN-γ. Alongside, 30-day exposure to this system could also significantly suppress tumor growth and expression of markers of tumor cell proliferation, angiogenesis, and metastasis, namely Ki-67, CD31, VEGFR2 and MMP-9.

Results: The number of tumor infiltrating lymphocytes (TILs), especially CD8+ T_h cells were significantly increased following exposure to ELF-EMF. Interestingly, pretreating cancer cells with N-acetyl cysteine, a free-radical scavenger, or verapamil, an L-type calcium channel blocker in vitro, could diminish observed necroptotic and apoptotic responses while pretreating with calcium chloride, could aggravate responses.

Conclusions: Overall, results of present study demonstrated that along with apoptosis, necroptosis is also a prominent form of cell death induced by exposure to ELF-EMF which is also dependent on elevated intracellular levels of ROS and calcium.

Background

Although modulatory effects of electromagnetic fields (EMFs) on living cells and tissues has long been documented *in vitro* and *in vivo*, our understanding from mechanisms of these interactions still remains in its infancy and far from being completely understood [1, 2]. In this context, recent studies on extremely low frequency electromagnetic fields (ELF-EMFs), produced by several household devices and industrial networks, have shown that these non-ionizing waves can affect multiple biological processes in living matter including expression of genes and proteins, as well as modulating physiological pathways governing cellular proliferation, differentiation or integrity either in direct or indirect ways [3–7].

Alongside, the therapeutic potential of ELF-EMF in treatment of cancer has long been documented *in vitro* and *in vivo* [8–11]. Regardless of few exceptions, ELF-EMF exposure promotes programmed cell death of cancer cells in vitro. Similarly, a tumor retardation response has been demonstrated in tumor bearing mice following exposure to ELF-EMF *in vivo* [8, 12–15]. More importantly, the advantage of this approach is its low damaging effects toward adjacent normal tissues. Therefore, many scientists have underscored the potential of ELF-EMF to be applied as an adjunctive therapy or even a primary therapeutic modality in treatment of cancer. Unfortunately, diversities in applied magnetic fields strengths, in addition to the lack of a generally accepted mechanism of action, has made it difficult to compare the results of exposure to ELF-EMF in different studies and come up with a unit treatment protocol.

Previously reported by Tatarov et al., 6 h/day exposure to a 100 mT, 1 Hz magnetic field for a total of 4-week period could successfully suppress breast tumor growth in nude mice [16]. Thus, in present study, was applied the same electromagnetic field to identify types of cancer cell's responses to ELF-EMF and studying underlying molecular and cellular pathways. Currently, induction of "apoptosis" is the main proposed explanation for anti-tumorigenic effects observed following exposure to ELF-EMF [17]. Apoptosis is a "caspase" dependent type of programmed cell death which is typically together with anti-inflammatory responses [18–20]. Very oddly however, we noticed a vigorous pro-inflammatory response *in vivo* with a very significant increase in serum TNF-α concentration following 6 h/day ELF-EMF exposure at the end of 40-day period which could not be simply explained by classical apoptotic pathway's characteristics. Similar results were also recorded when daily exposure time was reduced to 2 h/day though with less intensities. As these responses are typical characteristics of another type of programmed cell death, namely "necroptosis", we further investigated the possibility of necroptosis occurrence in response to ELF-EMF exposure. Finally, as ELF-EMF has shown to affect reactive oxygen species (ROS) formation and perturb intracellular calcium levels, we further investigated how modulation of these two factors can affect induction of necroptosis using their specific modulators.

Material And Methods

Cell lines

MC4-L2 Estrogen receptor-positive (ER^+) breast duct carcinoma cells [21] were obtained from Iranian Institute of Genetic Resources and maintained in DMEM/F-12 medium supplemented with 10% fetal bovine serum (FBS Gibco, Thermo Fisher, USA), 100 µg/ml streptomycin and 100 U/ml penicillin (Invitrogen, Burlington, ON) at 37°C in 5% CO_2.

Animals

Adult inbred Balb/C mice (~20-25 g) were obtained from Pasteur Institute of Iran (Tehran, Iran) and were housed in groups of five to six under regular 12 h light/dark cycles. Mice were allowed to access water and food freely and whole experiment was carried out between 10.00 A.M to 13 P.M each day using regular room light and temperature. All animal experiments were performed according to the ARRIVE guidelines and National Institutes of Health guide for the care and use of Laboratory animals (NIH Publications No. 8023, revised 1978). At the end of experiment, all mice were sacrificed by cervical dislocation. The Whole experiment, design of the study and included techniques were approved by the ethics committee of the Motamed Cancer Institute, ACECR, Iran.

EMF exposure systems

ELF-EMF exposure system applied herein was identical to the one previously described by our group [22]. The exposure device consisted of two couples of square coils in a U-shape solenoid like configuration and an ironic core which guaranties required homogeneity and maximizes B-field levels. Each mentioned coil has a side length equal to 2cm that is covered with 1250 single-strand copper wires. Coils were

positioned in a way that the shortest distance among their ends was equal to 15 cm. In order to obtain a tunable magnetic field within the range of 1–100 mT in intensity and 1–60 Hz in frequency, a wave form generator (GW Instek SFG-1000 Series, South Korea) was coupled to the coils. To minimize possible effects of ELF-EMF on control group, the incubator of ELF-EMF non-treated group (control group) was located in a place which received EMFs similar to those of background. Using a scope coupled parallel to a resistor in series with coils, waveforms, frequency and magnetic field intensity B were carefully monitored. The inhomogeneity close to the ironic plates edge was about 10%. Using a Lakeshore® Gauss meter, point by point calibration of the net-like plastic plate located at the bottom of exposure zone was performed and an 8 × 8 cm square at central part was determined as exposure zone where field alterations were less than 2%.

In vitro studies

Cell proliferation assay

Throughout the study, cells in passage number 3-4 were applied to minimize variations induced by different cellular characteristics. Cells were detached from flasks with the use of 0.025% Trypsin-EDTA after reaching an 80% confluency, and were then neutralized using 10% FBS and centrifugated. Following dispersion of pellets, Cells were seeded in 6-well plates with an initial density of 5×10^4 cells/well. Cells were exposed to 100 mT, 1 Hz magnetic fields daily for 2 h. Exposures continued for 5 consecutive days, the time equal to 2-3 population doubling time, and at the end of the fifth day, cells were detached using 0.025% Trypsin-EDTA and cell viability was measured according to trypan blue staining protocol. The percent of cell inhibitory effect following ELF-EMF treatment was calculated by dividing the differences between counted cells of sham and ELF-EMF exposed groups by total number of cells grown in sham group (formula 1):

$$\text{Percent of cell growth inhibition} = [(\text{Sham Group}_{\text{Number of cells}} - \text{ELF-EMF Group}_{\text{Number of cells}}) / \text{Sham Group}_{\text{Number of cells}}] \times 100$$

In some performed studies, in order to evaluate the role of intracellular ROS in ELF-EMF induced anti-proliferative effects, cells were pretreated with 2.5 mM N-acetyl cysteine (NAC), a potent scavenger and inhibitor of intracellular ROS accumulation 30 min prior to daily ELF-EMF exposures. In addition, to evaluate the role of Ca^{2+} concentrations on ELF-EMF induced effects, cells were pretreated with 5 mM calcium chloride, a precursor of calcium, or 10 μM verapamil, a potent inhibitor of L-type voltage gated channels 30 min prior to daily ELF-EMF exposure. Dosages applied in present study were chosen according to a preliminary screening test and were those which could induce desired biological effects without presenting significant cytotoxicity.

Flowcytometry analysis of programmed cell death

In order to evaluate probable induction of programmed cell death following exposure to ELF-EMF, MC4-L2 cell lines were seeded at a density of 5×10^5 cells/well in 6-well plates and exposed to 100 mT, 1Hz ELF-

EMFs 2h daily for 5 days. At the fifth day, cells were collected immediately after exposure and stained with annexin V/ propidium iodide kit prior to analysis on a Beckman Coulter FC500 cytometer. Similarly, for analyzing the role of ROS or Ca^{2+} on ELF-EMF mediated effects, cells were pretreated with reagents mentioned in previous section 30 min prior to daily exposures.

Intracellular reactive oxygen species detection

To evaluate changes in intracellular levels of reactive oxygen species (ROS) following exposure to ELF-EMF, cells were stained with 2', 7'-dichlorofluorescin diacetate (DCFH-DA, Sigma, US) fluorescent dye and then analyzed by flowcytometry. In brief, following ELF-EMF exposure, cell media were replaced with pre-warmed serum-free media containing 5 μM DCFH-DA and incubation continued for 30 min. Cells were then washed three times with PBS to remove extra DCFH-DA and detached using 0.25% trypsin-EDTA for fluorescent intensity measurement by flowcytometry. For each experiment, 10^4 cells were counted and read under flow cytometer. To obtain reliable results, each experiment was repeated at least three times. In some experiments, effect of NAC, calcium chloride and verapamil pretreatment on cellular ROS levels following exposure to ELF-EMF was also studied.

Fluorescence microscopic detection of calcium influx

The effects of ELF-EMF exposure on intracellular calcium levels was studied using FURA4-AM fluorescent die. In brief, on the fifth day of treatment, cells were incubated with FURA4-AM at a final concentration of 1 μM, 15 min prior to exposure to ELF-EMF. In some experiments, cells were also treated with NAC, calcium chloride or verapamil following incubation with FURA4-AM for 30 min prior to ELF-EMF exposure. Before ELF-EMF exposure, the fluorescence background associated with cells were recorded under an LSM510 inverted fluorescence microscope. At the end of the 2h exposure period, cells were again imaged and fluorescent intensities were determined using ImageJ software. Data were reported as mean± SD of arbitrary units of three independent experiments performed on different days.

Acridine orange staining

To evaluate the increase in number of AVOs, a hallmark of induction of autophagy, following exposure to ELF-EMF, MC-4L2 cells were stained with acridine orange fluorescent dye. In some experiments, cells were also treated with NAC, calcium chloride or verapamil 30 min prior to ELF-EMF exposure. In brief, following ELF-EMF exposure, cells were incubated with acridine orange with a final concentration of 5 μg/ml for 15 min and then green and red fluorescence were visualized utilizing an LSM510 inverted fluorescence microscope. Intensity of red fluorescence, as a response to AO accumulation in AVOs, was measured using ImageJ software and reported as mean ± SD of intensity of 3 independent experiments.

Western blot analysis

Following ELF-EMF exposure, cells were collected and homogenized using lysis buffer (10 mM Tris-Cl pH 7.4, 150 mM NaCl, 1% Triton-X100 and proteases inhibitor cocktail). Achieved cell lysates were than

subjected to centrifugation at 15,000 *g* for 30 min at 4 °C and supernatant was collected for further analysis. Proteins in supernatant were then separated by SDS-PAGE and transferred on a PVDF membrane for further visualization. Using a 5% bovine serum albumin, blotted PVDF membranes were blocked for 1 h and then probed using primary antibodies against caspase-3 (ab4051, Abcam), caspase-8 (ab25901, Abcam), caspase-9 (ab52298, Abcam), RIPK1 (sc-133102, Santa Cruz Biotechnology), phosphorylated RIPK1 (p-RIPK1) (#44590, CST), RIPK3 (#13526, CST), phosphorylated RIPK3 (p-RIPK3) (ab195117, Abcam, Cambridge, MA, United States), MLKL (ab172868, Abcam), phosphorylated MLKL (p-MLKL) (ab196436, Abcam) and GAPDH (sc-32233, Santa Cruz Biotechnology). Following addition of secondary antibodies and washing with TBST for 3 times, the immunoreactive bands were visualized utilizing a ChemiDoc XRS Image System (Bio-Rad Laboratories, Hercules, CA, USA). Obtained images were then quantified ImageJ analysis software.

In vivo studies

In vivo EMF exposure experiments in mice

14 mice were randomly divided in to two groups, each containing 7 mice, one receiving 100 mT, 1 Hz ELF-EMF 2h daily for a period of 28-day and the other receiving no treatment, serving as control group. For development of MC-4L2 tumors, 10^6 cells were subcutaneously injected to right flank of one mouse and allowed to growth for 3 weeks. Next, established tumor was dissected and minced in to several 1-2 mm^3 pieces under sterile condition. Each section was then subcutaneously grafted in to one mouse and allowed to grow up to a mean size of 150 mm^3. Following this point, exposures were initiated and continued up to 28 days. Mice were routinely monitored for possible cytotoxicity during the 28-day period and weighed every day using a digital balance. Tumor sizes were also measured every day using a digital caliper and tumor sizes were calculated using following formula:

$$\text{Tumor size } (mm^3) = ½ \times \text{length} \times (\text{width})^2$$

At the end of the 28-day treatment period, mice were sacrificed, their tumors were dissected, weighed and fixed in 4% paraformaldehyde for further analysis. The graph of tumor size growth as the function of time was drawn for both groups and compared with each other. Weight of tumors at the end of 28-day treatment period was also measure in both groups and compared with each other.

H&E staining and Immunohistochemistry

Tumors were dissected from mice bearing MC4-L2 tumors and fixed in 4% paraformaldehyde overnight. Fixed tumors were then dehydrated in an alcohol gradient, followed by paraffin-embedment and sectioning in to slices with a thickness of 4 μm. Following deparaffinization in xylene and rehydration, Hematoxylin and eosin (H&E) staining and immunohistochemistry (IHC) were performed based on a established protocol [23]. Primary antibodies utilized herein included anti-VEGFR2 (#2479L, CST), anti-MMP9 (#13667T, CST), anti-Ki67 (#9449T, CST), anti-CD31+ (#3528S, CST), anti-CD8+ (#85336S, CST) and anti-CD4+ (sc-13573 L, Santa Cruz Biotechnology). Following an overnight incubation with primary

antibodies, sections were carefully washed and incubated for about an hour with secondary antibody at room temperature. Sections were then visualized through staining with diaminobenzidine and nucleus counterstaining with hematoxylin. Images were taken from sections using an Olympus light microscope. Tumor infiltrating lymphocytes (TILs) number in H&E stained sections was also counted by an expert pathologist.

TUNEL assay

Following embedment in paraffin, tumor tissues were sectioned in to 4 μm slices and subjected to TUNEL assay using a commercially available detection kit (Biovision, Canada) according to the manufacturer's provided guideline. Following this step, each section was stained with diaminobenzidine and counterstained with hematoxylin. Images were taken using an LSM510 fluorescence microscope.

Multi-Analyte ELISArray for analyzing serum levels of inflammatory cytokine

At the end of the treatment period, mice blood samples were collected by heart puncture. Serum samples were immediately separated by centrifugation and stored at -80 °C until further analysis. A MEM-004A Multi-Analyte ELISArray Kit (Qiagen, US) was used for analyzing 12 inflammatory cytokines including IL-1α, IL-1β, IL-2, IL-4, IL-6, IL-10, IL-12, IL-17A, TNF-α, IFNγ, G-CSF and GM-CSF. Procedure was performed according to the manufacturer's provided instructions and data were represented as fold changes compared to non-treated control group.

Statistical analysis

For evaluation of statistical differences between two group, unpaired Student's *t*-test and for comparison of more than two groups one-way analysis of variances (ANOVA) with tukey's post hoc test was applied. Throughout the study, data were expressed as the mean ± the standard deviation of the mean (SD). Differences were considered significant when $P < 0.05$.

Results

Exposure to ELF-EMF induced a pro-inflammatory response in vivo resembling those of necroptosis

As depicted in Fig. 1A, both 2 h and 6 h/day exposure to ELF-EMF could effectively suppress tumor growth rate and final weight compared to non-exposed mice. Nevertheless, no significant differences in rate of tumor growth was observable between 2 h- and 6 h/day exposed groups at the end of 40-day treatment period which was contrary to the previous report by Tatarov et al. [16] Moreover, represented in Fig. 1B, TUNEL positive cells in ELF-exposed group were significantly higher in number compared to the non-treated group. Again, TUNEL positive cells in 2- and 6 h/day exposed group were not significantly different in number with each other. Strangely, in addition to classical highly dense bright blue spots, detectible in nuclei of apoptotic cells (representative of condensed DNA), an atypical smeared form of DNA with no changes in the nuclear figure or size and density of blue color was also observable in TUNEL positive cells. Whereas positive cells in TUNEL assay are usually considered as apoptotic cells due to the

presence of fragmented DNA, different studies have demonstrated that necrotic cells, either in its programmed form or the other, also possess fragmented DNA which can interact with TUNEL *in vivo*, and thus, can be considered as another marker for induction of a necroptotic response *in vivo* [24]. Also, examining H&E stained sections of ELF treated and non-treated groups, a significantly raised number of tumor infiltrated cells (TILs) was observable in both 2 h- and 6 h-/day exposed group compared to the control (Fig. 1C).

Identifying possible changes in profile of 12 pro-/anti-inflammatory cytokines in collected blood samples at the end of the treatment period, a vigorous pro-inflammatory response, evident from a very noticeable increase in TNF-α, IL-6 and IL-1β concentrations (~ × 3, × 2.7 and × 3 fold increase respectively) was detected following both 2 h and 6 h/day exposures to 100 mT, 1 Hz ELF-EMF (Fig. 2A). Similarly, concentrations of other pro-inflammatory cytokines including IL-2, IL-12 and IL-17A were also significantly raised. Notably, concentration of IFN-γ, an important cytokine with tumor suppressive effects, was also significantly raised while the concentration of pleiotropic anti-inflammatory cytokine IL-4 remained almost unchanged. This pro-inflammatory response was highly representative of those observed during necroptosis in vivo [25]. Based on previous reports, increased TNF-α concentration induces expression of several pro-inflammatory cytokines including IL-6, IL-1β, IL-17, etc. during a necroptotic response.

In parallel, secretion of specific molecules containing DAMPs from cell undergoing necroptosis and production of other cytokines including IL-1α react with neighboring cells and promotes antigen presenting cells (APC) recruitment and activation [26]. This further promotes initiation of an effective adaptive immune response. Consistent with these findings, as depicted in Fig. 2B, the number of tumor infiltrated lymphocytes was significantly increased compared to non-treated cells and the proportion of CD8 + T cells was significantly increased compared to the non-treated group which can be attributed to the specific pattern of secreted cytokines. These evidences, further potentiate the possibility of induction of a necroptotic response following ELF-EMF exposure.

Interestingly, despite of the significant increase in TNF-α and several other pro-angiogenic cytokines levels, the effect of treatment with ELF-EMF on MMP-9 and VEGFR2 expression, as well as the number of CD31 + cell in tumor site was dwindling, proposing a net anti-angiogenic effect on exposed mice (Fig. 2B). Similarly, previous reports have also demonstrated that *Ripk3*$^{-/-}$ mice undergo similar changes and the process of cutaneous wound healing becomes significantly impaired in them. What can be possibly proposed herein, is that very high concentration of TNF-α at site of action may have resulted in down-regulation of these receptors and had led to following consequences.

ELF-EMF exposure induces necroptosis and apoptosis programmed cell deaths in vitro

To further confirm the hypothesis of induction of necroptotic cell death by ELF-EMF, different in vitro cellular studies were performed. Mimicking chronically exposed condition *in vivo*, cells were exposed to the same ELF-EMF for 5 days, equivalent to about 3 population duplicating time of cells *in vitro* [27]. It is

almost accepted that ELF-EMF mediated biological effects are linked to calcium overload and ROS overproduction [28]. Consequently, we also examined whether these two factors could be involved in necroptotic like responses mediated by ELF-EMF exposure. To this end, in some experiments, cells were also treated with H_2O_2, a source for overproduction of ROS; n-acetyl cysteine (NAC), a potent ROS scavenger; verapamil, a potent L-type calcium (Ca^{2+}) channel blocker; or calcium chloride, a source for raised extracellular Ca^{2+} concurrent to the ELF-EMF exposure.

Initially, inhibitory effects of ELF-EMF exposure on MC4-L2 cell proliferation was evaluated by trypan blue staining. As depicted in Fig. 6A, exposure to ELF-EMF could significantly reduce the number of live cells compared to non-treated group. Interestingly, these inhibitory effects were completely abolished upon co-treatment of cells with NAC or verapamil while excess extracellular Ca^{2+} could potentiate anti-proliferative effects of ELF-EMF. In parallel, cells were also stained with annexin V and PI, and analyzed with flowcytometry. Generally, in necroptotic cell death, phosphatidyl serine is externalized prior to cell membrane penetration and secretion of necroptotic bodies [29]. Furthermore, similar to necrosis, PI can also internalize through disintegrated membrane of necroptotic cell and stain DNA. Thus, full necroptotic response can be understood from summing up PI (+)/AV (-) population, representing cells undergoing necrosis and PI (+)/AV (+) population, representing cells undergoing late necroptosis. However, the later population can also account for cells undergoing late apoptosis. Thus, AV/PI staining is not a highly selective test for differentiating apoptosis from necrosis. Despite this, during apoptosis, an increase in both early and late apoptotic subpopulations is expected and if late apoptosis is suddenly raised while early apoptosis remained intact means that other forms of programmed cell death including necroptosis may also be involved. As depicted in Fig. 6A, ELF-EMF treatment could significantly increase double AV/PI positive and AV positive PI negative subpopulation of cells which is indicative of induction of apoptosis, necroptosis or both. Despite this, only a trivial increase in number of PI-/AV + cells was observable following exposure to ELF which is highly representative of necroptotic cell death rather than apoptotic one. Similarly, co-treatment with NAC and verapamil could significantly reduce number of cell deaths while excess Ca^{2+} could aggravate the results.

To further illustrate the nature of the programmed cell death, western blot analysis was performed for identification of changes induced in protein levels of pro-caspase 3, cleaved caspase 3, procaspase 9, cleaved caspase 9 and procaspase 8, cleaved caspase 8, following exposure to ELF-EMF. As illustrated in Fig. 3, concentrations of cleaved caspase − 9, -3 and − 8 were significantly increased following ELF-EMF exposure, highly proposing that ELF-EMF induces apoptosis through both intrinsic and extrinsic pathways. Interestingly, co-treating cells with verapamil could significantly reduce amounts of cleaved caspase − 3, -8 -9 upon exposure to ELF while co-treating cells with NAC could only significantly suppress cleavage of caspase − 9 while amounts of cleaved caspase − 3 and − 9 remained almost unchanged. With this data in mind, one can hypothesize that ROS overproduction upon ELF exposure is part of the scenario behind ELF-EMF exposure induced apoptosis and rather, calcium overload, as antagonized upon co-treating with verapamil may be the prevalent event in induction of apoptosis. Oddly however, upon introducing excess calcium into the extracellular environment and exposing to ELF-EMF, no significant

enhancement in cleaved caspases − 3, -9 and − 8 in comparison to ELF-EMF exposure alone was observed while flowcytometry analysis demonstrated a significant increase in number of late apoptotic population upon co-treating with calcium chloride compared to ELF-EMF alone. Thus, calcium overload may have increased number of AV+/PI + population with a cell death pattern independent from apoptosis (Fig. 6A). As necroptosis can also increase the number of cells in this subpopulation and considering data obtained from in vivo studies, we hypothesized that ELF-EMF exposure may induce calcium overload with in turn, can trigger cell death by necroptosis. This hypothesis become stronger considering previous reports in literature, proposing necroptosis as an event strongly dependent on calcium overload together with manifestation of ROS overproduction. Recently it has been shown that ROS overproduction may result in auto phosphorylation of RIPK-1, the initiator of necroptosis cascade [30]. It seems that exposure to ELF-EMF could result in similar cascade of events.

To confirm occurrence of necroptosis as another form of programmed cell death following ELF-EMF exposure, fold changes in protein levels of RIPK1, p-RIPK1, RIPK3, p-RIPK3, MLKL and p-MLKL was examined following exposure to ELF-EMF and co-treatment with calcium chloride, NAC and verapamil. As was expected, levels of p-RIPK1, p-RIPK3 and p-MLKL were significantly raised following ELF-EMF exposure alone and calcium chloride co-treated group (Fig. 4) while no significant changes were observable in other treatment groups. Based on these data, we concluded that calcium overload following ELF-EMF exposure can induce necroptotic cell death in addition to apoptosis.

Elf-emf Exposure Induces Necroptotic-like Morphological Alterations In Mc4-l2 Cells

To further illustrate the specific mode of cell death in MC4-L2 cell lines following ELF-EMF exposure, changes in cellular morphology was investigated by transmission electron microscopy (TEM). TEM images obtained from normal MC4-L2 cells demonstrated well-preserved cytoplasmic organelles, as well as smoothly shaped nuclei encompassing heterochromatin shaped chromatin (Fig. 5). Contrarily, H_2O_2 treated cells were used as apoptosis control group. This group of cells were mostly characterized by a marginated chromatin and formation of budding vesicles in the absence of swollen organelles. Upon examining ELF-EMF treated cells, in addition to the cells with typical apoptotic morphology, a large part of the cells demonstrated a translucent cytoplasm (yellow arrows), associated with disintegrated membrane (Blue arrow), organelle swelling (Red arrow) and condensed chromatin (Green arrow); all of which are typical characteristics of a necroptotic like cell death [31]. The most prevalent form of morphological changes in other groups was either apoptotic form (NAC co-treated) or normal form (NAC control, verapamil control and verapamil co-treated groups).

ROS overproduction and Ca $^{2+}$ overload interplay following ELF-EMF exposure is responsible for necroptotic events in MC4-L2 cell lines in vitro

DCHF-DA and FURA-4AM staining were used to evaluate possible enrolment of ROS and calcium in induction of ELF-EMF mediated necroptosis respectively. The mean fluorescent intensity of each group in DCHF-DA experiment was measured by flowcytometry and for FURA-4AM experiment was obtained by ImageJ software. Based on results, ELF-EMF exposure could significantly increase both ROS and intracellular Ca^{2+} levels in treated cells (Fig. 6B and D). Interestingly, while NAC co-treatment could only suppress ELF-EMF mediated ROS overproduction, calcium chloride co-treatment could enhance both intracellular overproduction of ROS and calcium overload simultaneously. These findings were extremely helpful in understanding the interconnection of ROS and calcium in development of ELF-EMF mediated necroptosis as blockade of ROS overproduction in the presence of intracellular calcium overload could suppress development of necroptosis while induction of ROS overproduction and calcium overload by calcium chloride co-treatment could induce necroptosis without having net effect on apoptosis. Furthermore, blockade of both calcium and ROS overload by verapamil could completely diminish both necroptosis and apoptosis induced by ELF-EMF. This strongly suggests that increase in intracellular calcium levels may happen following elevation of ROS overproduction.

ELF-EMF exposure induces autophagic response which is dependent on elevation of intracellular ROS concentration

To evaluate autophagic responses following ELF-EMF exposure, cells were stained with AO/PI fluorescent dyes. As depicted in Fig. 6C, exposure to ELF-EMF resulted in a significant increase in number of acidic vesicular organelles including lysosomes and autophagosomes which are depicted by orange dots in cytoplasmic region of cells. To evaluate the putative role of ROS and Ca2 + in autophagic response, cells were again pretreated with NAC, calcium chloride and verapamil. Interestingly, only administration of NAC could significantly reduce the number of autophagosomes and no significant differences were observed in autophagosome content of cells pretreated with calcium chloride and verapamil following exposure to ELF-EMF in comparison to cells which were only treated with ELF-EMF. Thus, it can be concluded that elevated intracellular ROS play a more important role in induction of autophagy in response to exposure to ELF-EMF.

ELF-EMF exposure induced caspase-independent program cell death is not in association with autophagic response

Comparing data obtained from autophagy responses with those related to caspase-independent program cell death didn’t demonstrate a direct relation between the intensity of autophagic response and the extension of caspase independent programmed cell death observed. The important point noticed herein was that although administration of verapamil couldn’t significantly decrease observed autophagic response, it could completely reverse caspase independent programmed cell death. Despite of a clear relation between increased autophagy and induction of necroptosis, this pattern didn’t happen in our case.

Discussion

To our best knowledge, this is the first study providing evidence for ELF-EMF mediated necroptotic cell death, which is different from currently accepted apoptosis hypothesis worldwide. Necroptotic cell death was initially suspected from vigorous inflammatory responses and appraisal of TNF-α concentration *in vivo*; beyond secretion of DAMPs as a result of cytoplasmic membrane disintegration, necroptosis have shown to promote pro-inflammatory responses through activation of expression of a vast number of genes. In this context, large part of up-regulated genes, including pro-inflammatory cytokines, are similar to those activated by TNFα pathway but at higher levels. Overexpression of pro-inflammatory cytokines seems to be a common characteristic of necroptosis as necroptosis stimulators other than TNFα including TRAIL can also significantly increase their expression. Finally, it has been suggested that overproduction of cytokines in TNFα-induced necroptosis takes place in a manner independent from DAMPs release and is highly dependent on NF-κB and p38 activation [32].

Necroptosis hypothesis was further confirmed by observation of a significant increase in phosphorylated levels of RIPK1, RIPK3 and MLKL proteins in parallel to a negligible change in cleaved caspase-3 level following exposure to ELF-EMF. This was concurrently associated with a significant increase in formation of autophagosomes and induction of autophagy, evident from an increase in the intensity of orange color emitted by acridine orange upon accumulation in acidic vacuoles. Interestingly, no significant changes in autophagic responses were observable following pretreatment with calcium chloride and verapamil in exposed cells while NAC could significantly attenuate autophagy both at the baseline and following ELF-EMF treatment in comparison to non-treated group. These data in first line suggests that autophagy may be an executor for ELF-EMF mediated necroptotic cell death and in second line, Ca^{2+} may very mildly be involved in autophagic responses and ROS may be the main executor in this context.

Although it is not completely clear how autophagy and necroptosis are interconnected in induction of cell death, a few studies have pointed out such relationship following treatment with specific agents. For instance, in the study performed by Yu et al. on L929 fibroblast cell line, treatment with zVAT, a pan caspase inhibitor, could initiate a cell death response characterized by formation of autophagosomic vacuoles. They demonstrated that inhibition of RIPK1, ATG7 or Beclin-1 expression could inhibit cell death and concluded that activation of mentioned genes involved in autophagy, are associated with necroptotic cell death and activation of caspases (presumably caspase 8) can suppress autophagic cell death [33]. Other studies have shown that T-cell activation results in formation of a DISC-like complex formed from assembly of FADD caspase-8 and RIPK1 on autophagosomic membranes [34]. This model strongly suggests that a certain level of autophagy is necessary for physiological proliferation of T-cells and manipulation of each of these components can affect proliferation. For instance, deletion of FADD and caspase-8 has shown to enhance autophagy and inhibit proliferation of T cells while inhibition of RIPK1 could restore proliferation of T-cells lacking normal FADD functionality. Recently it has been discovered that knocking out RIPK3 can also restore T cell proliferation [35]. Thus, it is possible that unregulated necroptosis and autophagy may induce T-cell death during clonal expansion and regulation of caspase 8 may have an important role in modulation of T-cell proliferation.

Monitoring intracellular calcium concentrations in different exposed groups, we demonstrated that cytoplasmic Ca^{2+} overload per se is not effective in induction of necroptosis. Consistent with numerous previously existing reports, pointing out enhancing effects of ELF-EMF on intracellular Ca^{2+} concentration, here we observed an increase in Ca^{2+} concentration following ELF-EMF exposure. Among co-treatment strategies for understanding the main players of ELF-EMF mediated necroptosis, only calcium chloride could enhance necroptosis which upon molecular examination, could significantly rise both intracellular ROS and calcium levels. Since NAC co-treatment could significantly reduce necroptosis event, evident from reduced p-MLKL compared to ELF-EMF group in western blotting and also flowcytometric analysis of AV+/PI + and AV-/PI + subpopulations, one can conclude that existence of ROS overproduction is essential in parallel to calcium overload for induction of necroptosis.

Different studies have pointed out that the role of ROS overproduction in induction of necroptosis may be cell dependent. For instance, it has been shown that in mouse embryonic fibroblast cells, TNF-α and BV6 induced necroptosis mainly takes place by RIP1- induced accumulation of ROS [36]. Similarly, based on Vanlangenaker et al. the main mechanism of Inhibitor of Apoptosis (cIAP)1induced anti-necroptotic event is suppression of RIP1-/RIP3- induced ROS overproduction [37]. Also, in an animal model of tuberculosis infection, TNF-α could accelerate mitochondrial ROS overproduction in mycobacteria infected macrophages by activating RIPK1/ RIPK3 pathway [38]. Contrarily however, in HT29 colon carcinoma cells or human monocyte-derived cell line THP-1, application of ROS scavengers couldn't reverse TNF-α induced necroptosis [39, 40]. Based on our results, necroptosis in MC4-L2 cell line may be activated upon accumulation of overproduced ROS in response to ELF-EMF exposure. Furthermore, overproduction of TNF-α in vivo upon exposure to ELF-EMF and accumulation of intracellular ROS may have been the underlying mechanism of induction of necroptosis. However, further studies for clarification of the underlying mechanism is highly recommended.

Calcium mediated necroptosis has also been discovered in *Caenorhabditis elegans*. In this context, hyperactivating MEC-4 ion channel by mutation, results in influx and accumulation of calcium up to a toxic level in *C. elegans* which can in turn, induce necroptotic neurodegeneration. Similarly, treating L929 cell lines with TNF-α results in appraisal of cytoplasmic calcium and induction of necroptosis [41, 42]. In addition, application of calcium chelators in L929 cells can completely diminish necroptosis, proposing an executive role for calcium in necroptosis [43]. Studies on HT29 cells have also demonstrated that following induction of necroptosis by TNF-α treatment, translocation of MLKL to the cytoplasmic membrane induces a vigorous calcium influx through the TPRM7, a non–voltage-sensitive ion channel ion channel, that is an early characteristic of necroptosis [44]. Notably, this ion channel functions downstream of MLKL and its knocking down doesn't have any effect on MLKL phosphorylation and trimerization. Consistently, here we demonstrated that application of verapamil, an antagonist of voltage gated calcium channels could diminish necroptosis while co-treating with calcium chloride aggravated it. Possible effect of verapamil may be the lessening of net calcium influx and calcium chloride effect may be potentiation of calcium influx through TPRM7 ion channels. However, further studies are highly recommended for proving correctness of this statement.

Conclusion

Overall, herein we confirmed that ELF-EMF exposure can induce tumor suppressing effects in vivo which is characterized by a significant increase in pro-inflammatory cytokines, most importantly TNF-α. In vitro studies also confirmed that ELF-EMF treatment induced cell death is not merely mediated by apoptosis. Necroptosis is another form of programmed cell death which is activated by ELF-EMF exposure and may be the underlying reason for the significant pro-inflammatory responses observed in vivo. Furthermore, in the context of MC4-L2 cell lines, both ROS accumulation and calcium overload are critical for induction of ELF-EMF mediated necroptosis. Finally, as recent studies have shown that necroptosis may be a good solution for treatment of cell lines resistant to chemotherapies, application of ELF-EMF in treatment of chemo-resistant cancers may become of great interest.

Abbreviations

EMFs
effects of electromagnetic fields
ELF-EMFs
extremely low frequency electromagnetic fields
ROS
reactive oxygen species
ER^+
Estrogen receptor-positive
NAC
N-acetyl cysteine
DCFH-DA
2', 7'-dichlorofluorescin diacetate
H&E
Hematoxylin and eosin
IHC
immunohistochemistry
TILs
Tumor infiltrating lymphocytes
ANOVA
analysis of variances
SD
standard deviation
APC
antigen presenting cells
TEM
transmission electron microscopy

Declarations

- **Ethics approval and consent to participate**

The project was found to be in accordance to the ethical principles and the national norms and standards for conducting medical research in Iran. Approved ID: IR.ACECR.IBCRC.REC.1394.42. Evaluated by Motamed Cancer Institute-Academic Centre for Education, Culture and Research. This institution performs its reviews based on United States Public Health Service (USPHS) regulations and applicable federal and local laws.

- **Consent for publication**

Not applicable.

- **Availability of data and material**

Not applicable.

- **Competing interests**

The authors declare no competing interests.

- **Funding**

This project has been funded by medical branch of Academic Center for Education, Culture and Research (ACECR), Tehran, Iran.

- **Authors' contributions**

AMA, MAJ, BD, SPS, LF and MS designed and supervised the study; MB and RG performed the most of experiments; Besides, TK, HS and HoS participated in animal investigations; ZSMM provided technique supports. Also, BD drafted and embellished the manuscript. All authors have read and approved the final manuscript

- **Acknowledgements**

Corresponding author highly acknowledges Motamed Cancer Institute for its facilities and specially, Prof. Keivan Majidzadeh-A for supporting us.

References

1. Saliev T, Begimbetova D, Masoud A-R, Matkarimov B. Biological effects of non-ionizing electromagnetic fields: Two sides of a coin. Progress in biophysics molecular biology. 2019;141:25–36.

2. Bergandi L, Lucia U, Grisolia G, Granata R, Gesmundo I, Ponzetto A, et al. The extremely low frequency electromagnetic stimulation selective for cancer cells elicits growth arrest through a metabolic shift. Biochimica et Biophysica Acta (BBA)-Molecular Cell Research. 2019;1866(9):1389–97.
3. Von Niederhäusern N, Ducray A, Zielinski J, Murbach M, Mevissen M. Effects of radiofrequency electromagnetic field exposure on neuronal differentiation and mitochondrial function in SH-SY5Y cells. Toxicol In Vitro. 2019;61:104609.
4. Cichon N, Saluk-Bijak J, Miller E, Sliwinski T, Synowiec E, Wigner P, et al. Evaluation of the effects of extremely low frequency electromagnetic field on the levels of some inflammatory cytokines in post-stroke patients. J Rehabil Med. 2019;51(11):854–60.
5. Oladnabi M, Bagheri A, Kanavi MR, Azadmehr A, Kianmehr A. Extremely low frequency-pulsed electromagnetic fields affect proangiogenic-related gene expression in retinal pigment epithelial cells. Iranian journal of basic medical sciences. 2019;22(2):128.
6. Hosseinabadi MB, Khanjani N, Samaei SE, Nazarkhani F. Effect of long-term occupational exposure to extremely low-frequency electromagnetic fields on proinflammatory cytokine and hematological parameters. Int J Radiat Biol. 2019;95(11):1573–80.
7. Consales C, Panatta M, Butera A, Filomeni G, Merla C, Carrì MT, et al. 50-Hz magnetic field impairs the expression of iron-related genes in the in vitro SOD1G93A model of amyotrophic lateral sclerosis. Int J Radiat Biol. 2019;95(3):368–77.
8. de Seze R, Tuffet S, Moreau JM, Veyret B. Effects of 100 mT time varying magnetic fields on the growth of tumors in mice. Bioelectromagnetics: Journal of the Bioelectromagnetics Society, The Society for Physical Regulation in Biology and Medicine. The European Bioelectromagnetics Association. 2000;21(2):107–11.
9. Novikov VV, Novikov GV, Fesenko EE. Effect of weak combined static and extremely low-frequency alternating magnetic fields on tumor growth in mice inoculated with the Ehrlich ascites carcinoma. Bioelectromagnetics: Journal of the Bioelectromagnetics Society, The Society for Physical Regulation in Biology and Medicine, The European Bioelectromagnetics Association. 2009;30(5):343 – 51.
10. Williams CD, Markov MS, Hardman WE, Cameron IL. Therapeutic electromagnetic field effects on angiogenesis and tumor growth. 2001.
11. Tofani S, Cintorino M, Barone D, Berardelli M, De Santi MM, Ferrara A, et al. Increased mouse survival, tumor growth inhibition and decreased immunoreactive p53 after exposure to magnetic fields. Bioelectromagnetics. 2002;23(3):230–8.
12. Cameron IL, Sun L-Z, Short N, Hardman WE, Williams CD. Therapeutic Electromagnetic Field (TEMF) and gamma irradiation on human breast cancer xenograft growth, angiogenesis and metastasis. Cancer Cell Int. 2005;5(1):23.
13. Liang Y, Hannan JC, Chang BK, Schoenlein PV. Enhanced potency of daunorubicin against multidrug resistant subline KB-ChR-8-5-11 by a pulsed magnetic field. Anticancer research. 1997;17(3C):2083–

8.

14. Omote Y, Hosokawa M, Komatsumoto M, Namieno T, Nakajima S, Kubo Y, et al. Treatment of experimental tumors with a combination of a pulsing magnetic field and an antitumor drug. Japanese journal of cancer research. 1990;81(9):956–61.
15. Zhang X, Zhang H, Zheng C, Li C, Zhang X, Xiong W. Extremely low frequency (ELF) pulsed-gradient magnetic fields inhibit malignant tumour growth at different biological levels. Cell Biol Int. 2002;26(7):599–603.
16. Tatarov I, Panda A, Petkov D, Kolappaswamy K, Thompson K, Kavirayani A, et al. Effect of magnetic fields on tumor growth and viability. Comp Med. 2011;61(4):339–45.
17. Santini M, Ferrante A, Rainaldi G, Indovina P, Indovina P. Extremely low frequency (ELF) magnetic fields and apoptosis: a review. Int J Radiat Biol. 2005;81(1):1–11.
18. Voll RE, Herrmann M, Roth EA, Stach C, Kalden JR, Girkontaite I. Immunosuppressive effects of apoptotic cells. Nature. 1997;390(6658):350–1.
19. Falasca L, Iadevaia V, Ciccosanti F, Melino G, Serafino A, Piacentini M. Transglutaminase type II is a key element in the regulation of the anti-inflammatory response elicited by apoptotic cell engulfment. J Immunol. 2005;174(11):7330–40.
20. Amarilyo G, Verbovetski I, Atallah M, Grau A, Wiser G, Gil O, et al. iC3b-opsonized apoptotic cells mediate a distinct anti-inflammatory response and transcriptional NF-κB-dependent blockade. Eur J Immunol. 2010;40(3):699–709.
21. Lanari C, Lüthy I, Lamb CA, Fabris V, Pagano E, Helguero LA, et al. Five novel hormone-responsive cell lines derived from murine mammary ductal carcinomas: in vivo and in vitro effects of estrogens and progestins. Cancer research. 2001;61(1):293–302.
22. Ansari AM, Majidzadeh-A K, Darvishi B, Sanati H, Farahmand L, Norouzian D. Extremely low frequency magnetic field enhances glucose oxidase expression in Pichia pastoris GS115. Enzym Microb Technol. 2017;98:67–75.
23. Tian J, Jiao X, Wang X, Geng J, Wang R, Liu N, et al. Novel effect of methionine enkephalin against influenza A virus infection through inhibiting TLR7-MyD88-TRAF6-NF-κB p65 signaling pathway. Int Immunopharmacol. 2018;55:38–48.
24. Kraupp BG, Ruttkay-Nedecky B, Koudelka H, Bukowska K, Bursch W, Schulte-Hermann R. In situ detection of fragmented DNA (TUNEL assay) fails to discriminate among apoptosis, necrosis, and autolytic cell death: a cautionary note. Hepatology. 1995;21(5):1465–8.
25. Kearney CJ, Martin SJ. An inflammatory perspective on necroptosis. Molecular cell. 2017;65(6):965–73.
26. Land WG. The role of damage-associated molecular patterns (DAMPs) in human diseases: part II: DAMPs as diagnostics, prognostics and therapeutics in clinical medicine. Sultan Qaboos University Medical Journal. 2015;15(2):e157.
27. Farina M, Farina M, Mariggio MA, Pietrangelo T, Stupak JJ, Morini A, et al. ELF-EMFs induced effects on cell lines: Controlling ELF generation in laboratory. Progress In Electromagnetics Research.

2010;24:131–53.

28. McLeod KJ, Rubin CT, Donahue HJ, Guilak F, editors. On the mechanism of extremely low frequency (ELF) electric field interactions with living tissue. [1992] Proceedings of the Eighteenth IEEE Annual Northeast Bioengineering Conference; 1992: IEEE.
29. Zargarian S, Shlomovitz I, Erlich Z, Hourizadeh A, Ofir-Birin Y, Croker BA, et al. Phosphatidylserine externalization,"necroptotic bodies" release, and phagocytosis during necroptosis. PLoS Biol. 2017;15(6):e2002711.
30. Ni H-M, McGill MR, Chao X, Woolbright BL, Jaeschke H, Ding W-X. Caspase inhibition prevents tumor necrosis factor-α–induced apoptosis and promotes necrotic cell death in mouse hepatocytes in vivo and in vitro. Am J Pathol. 2016;186(10):2623–36.
31. Degterev A, Huang Z, Boyce M, Li Y, Jagtap P, Mizushima N, et al. Chemical inhibitor of nonapoptotic cell death with therapeutic potential for ischemic brain injury. Nature chemical biology. 2005;1(2):112–9.
32. Zhu K, Liang W, Ma Z, Xu D, Cao S, Lu X, et al. Necroptosis promotes cell-autonomous activation of proinflammatory cytokine gene expression. Cell death disease. 2018;9(5):1–16.
33. Yu L, Alva A, Su H, Dutt P, Freundt E, Welsh S, et al. Regulation of an ATG7-beclin 1 program of autophagic cell death by caspase-8. Science. 2004;304(5676):1500–2.
34. Bell BD, Leverrier S, Weist BM, Newton RH, Arechiga AF, Luhrs KA, et al. FADD and caspase-8 control the outcome of autophagic signaling in proliferating T cells. Proceedings of the National Academy of Sciences. 2008;105(43):16677-82.
35. Lu JV, Weist BM, Van Raam BJ, Marro BS, Nguyen LV, Srinivas P, et al. Complementary roles of Fas-associated death domain (FADD) and receptor interacting protein kinase-3 (RIPK3) in T-cell homeostasis and antiviral immunity. Proceedings of the National Academy of Sciences. 2011;108(37):15312-7.
36. Lin Y, Choksi S, Shen H-M, Yang Q-F, Hur GM, Kim YS, et al. Tumor necrosis factor-induced nonapoptotic cell death requires receptor-interacting protein-mediated cellular reactive oxygen species accumulation. J Biol Chem. 2004;279(11):10822–8.
37. Vanlangenakker N, Bertrand M, Bogaert P, Vandenabeele P, Berghe TV. TNF-induced necroptosis in L929 cells is tightly regulated by multiple TNFR1 complex I and II members. Cell death disease. 2011;2(11):e230-e.
38. Roca FJ, Ramakrishnan L. TNF dually mediates resistance and susceptibility to mycobacteria via mitochondrial reactive oxygen species. Cell. 2013;153(3):521–34.
39. Temkin V, Huang Q, Liu H, Osada H, Pope RM. Inhibition of ADP/ATP exchange in receptor-interacting protein-mediated necrosis. Molecular cellular biology. 2006;26(6):2215–25.
40. He S, Wang L, Miao L, Wang T, Du F, Zhao L, et al. Receptor interacting protein kinase-3 determines cellular necrotic response to TNF-α. Cell. 2009;137(6):1100–11.
41. Bianchi L, Gerstbrein B, Frøkjær-Jensen C, Royal DC, Mukherjee G, Royal MA, et al. The neurotoxic MEC-4 (d) DEG/ENaC sodium channel conducts calcium: implications for necrosis initiation. Nature

neuroscience. 2004;7(12):1337–44.

42. Xu K, Tavernarakis N, Driscoll M. Necrotic cell death in C. elegans requires the function of calreticulin and regulators of Ca2 + release from the endoplasmic reticulum. Neuron. 2001;31(6):957–71.
43. Festjens N, Berghe TV, Vandenabeele P. Necrosis, a well-orchestrated form of cell demise: signalling cascades, important mediators and concomitant immune response. Biochimica et Biophysica Acta (BBA)-Bioenergetics. 2006;1757(9–10):1371–87.
44. Cai Z, Jitkaew S, Zhao J, Chiang H-C, Choksi S, Liu J, et al. Plasma membrane translocation of trimerized MLKL protein is required for TNF-induced necroptosis. Nat Cell Biol. 2014;16(1):55–65.

Figures

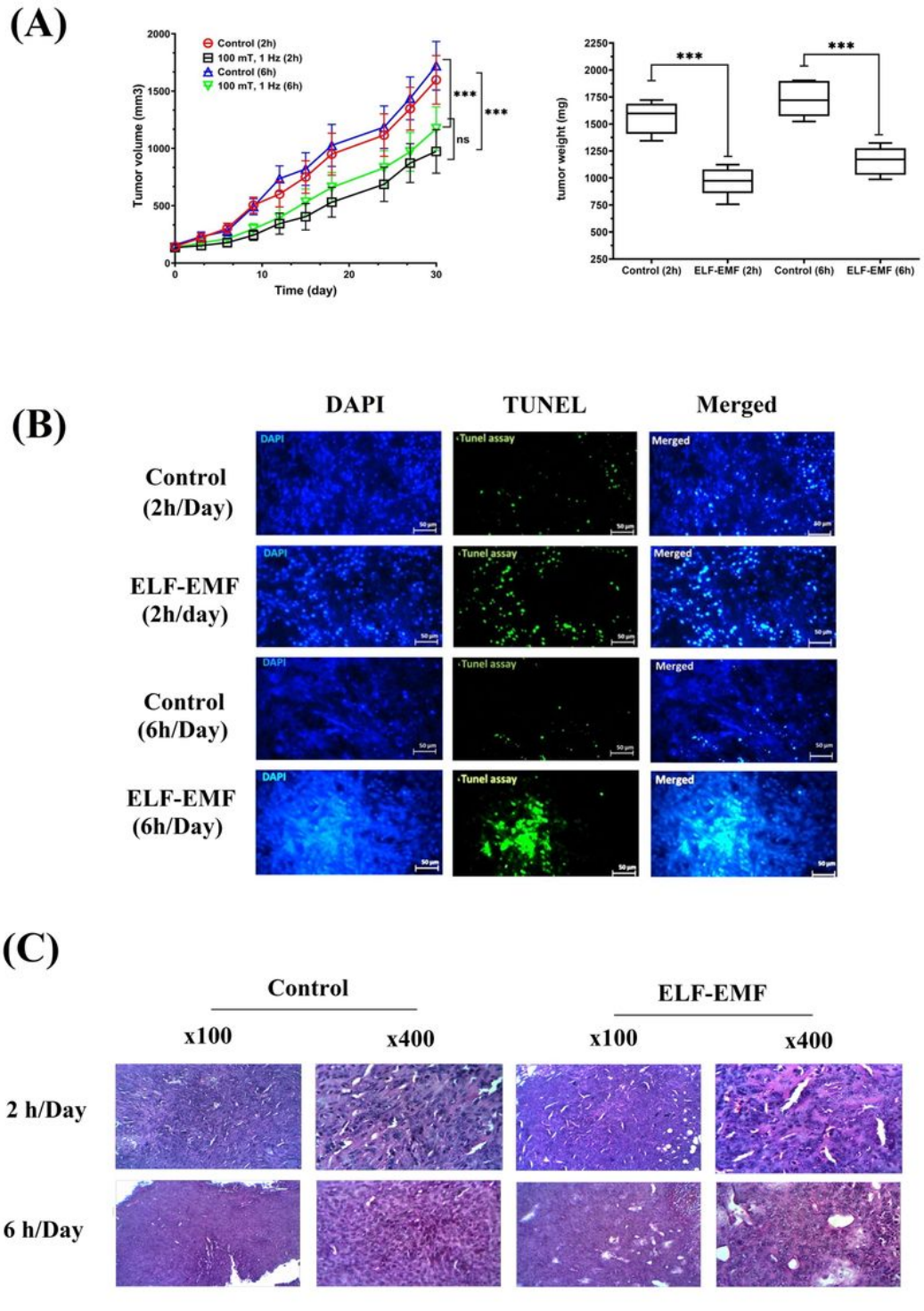

Figure 1

ELF-EMF exposure could effectively suppress tumor growth in vivo and enhance tumor infiltrated cell (TIL) number in treated mice. (A) Left panel: 2h- and 6h/day exposure to ELF-EMF for a 30-day period could effectively reduce tumor growth rate. No differences however were not observable in tumor growth rate between two treated groups. Right panel: tumor weights at the end of treatment period was significantly lower in ELF exposed group compared to the non-exposed control ones. (B) Tunnel assay,

demonstrating a significantly higher number of cells with fragmented DNA (green fluorescent) for both ELF-EMF exposed groups compared to their non-treated counterparts. Note the differences between the shapes of nuclei in ELF-EMF treated groups (low brightness, not condensation and presence in smeared form) and their controls (highly condensed blue color). (C) H&E staining of tumor sections at the end of treatment period, demonstrating a significantly increased number of TILs in tumor site compared to non-exposed specimen.

Figure 2

Exposure to ELF-EMF induces a pro-inflammatory response in vivo. (A) examining profile of 12 pro/anti-inflammatory cytokines using ELISA technique demonstrated a significant increase in majority of inflammatory cytokines, including IFN-γ (5× folds), TNF-α (3×folds), IL-6 (×3 fold) and IL-1β (×3 folds) in ELF-EMF exposed groups. Note that 6h exposure could more effectively induce inflammatory responses compared to the 2h/day treatment regimen. (B) IHC staining of tumor sections also demonstrated a significant decline in expression of angiogenesis (VEGFR2, MMP9 and CD31), proliferation markers (Ki-67). Contrarily the number of CD8+ cells significantly raised following ELF-EMF exposure to ELF-EMF treatment. Also, exposure to ELF-EMF treatment reduced ER and Her2 expression levels at the end of treatment, while results of 2h and 6h/day exposure was conflicting on PR expression. These results highly suggest the importance of patients monitoring during the time of ELF-EMF adjuvant therapy.

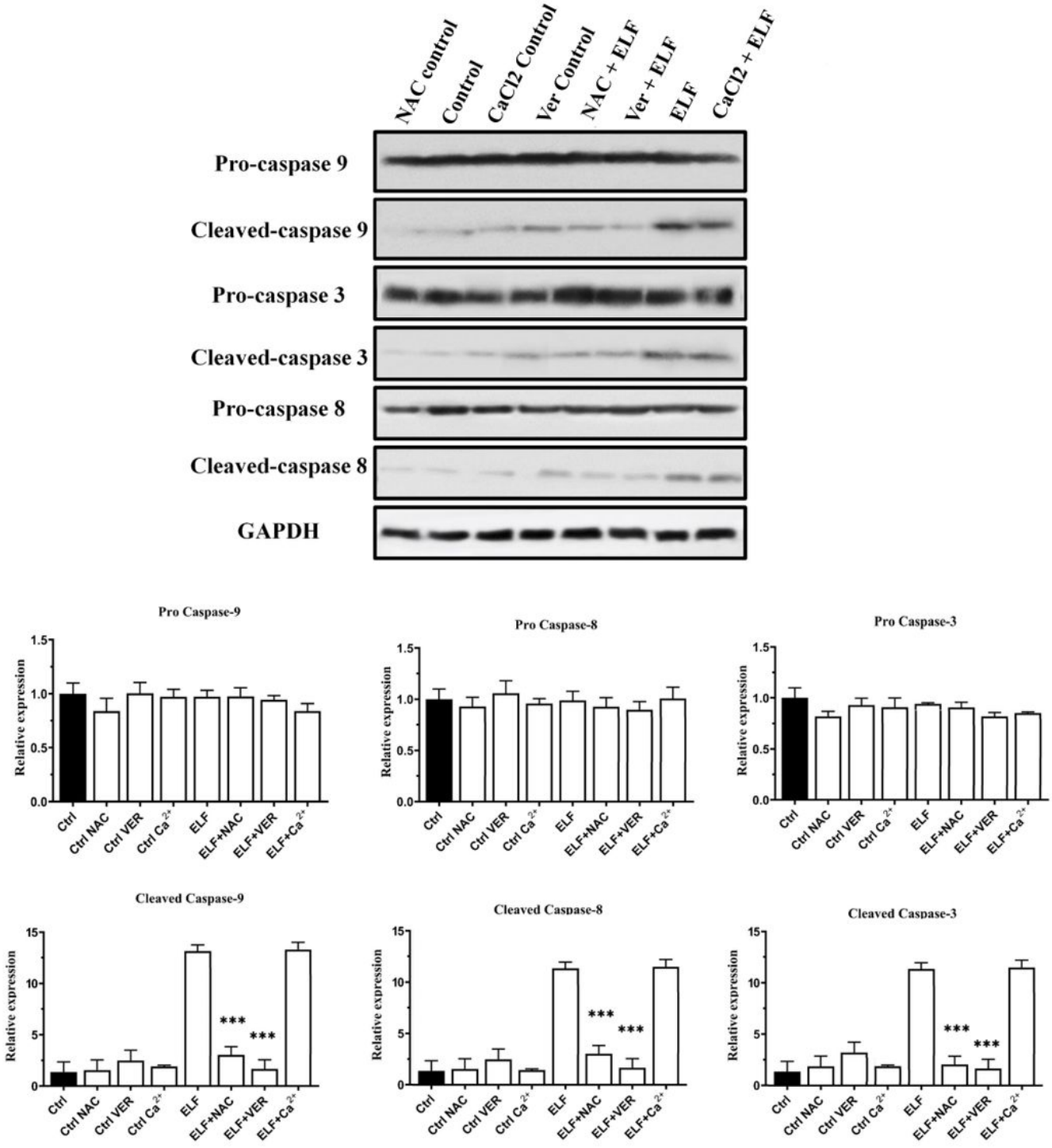

Figure 3

ELF-EMF exposure can induce apoptotic cell death in vitro. ELF-EMF exposure significantly increased concentrations of cleaved caspase -9, -3 and -8, proposing that ELF-EMF can induce apoptosis through both intrinsic and extrinsic pathways. Meanwhile, co-treating cells with verapamil could significantly reduce amounts of cleaved caspase -3, -8 -9 upon exposure to ELF while co-treating cells with NAC could only suppress cleavage of caspase -9. Finally, introducing excess calcium into the extracellular

environment of cells and exposing them to ELF-EMF, did not significantly enhance amounts of cleaved caspases -3, -9 and -8 in comparison to ELF-EMF exposure alone.

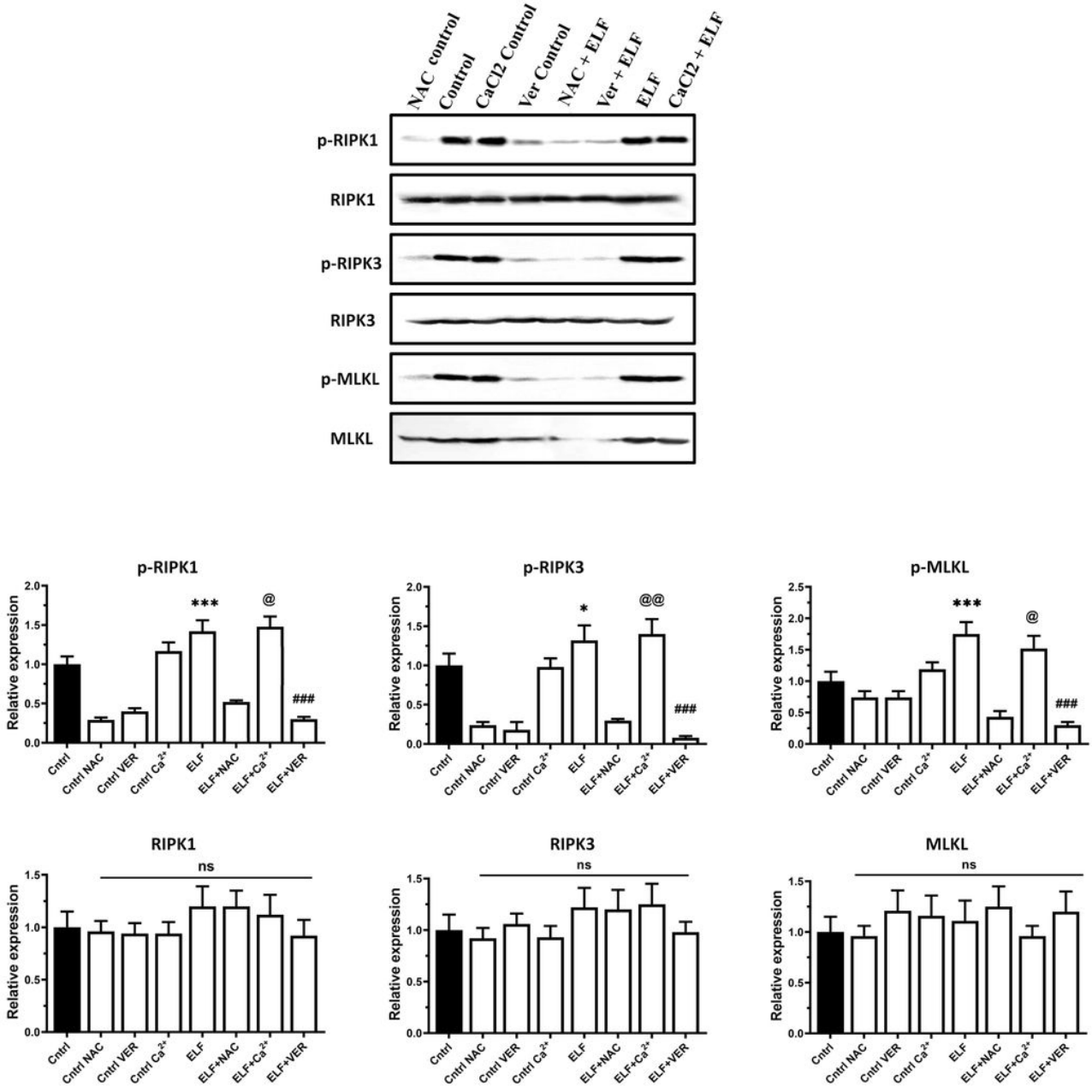

Figure 4

ELF-EMF exposure can induce necroptosis in vitro. Levels of p-RIPK1, p-RIPK3 and p-MLKL were only significantly raised following ELF-EMF exposed and calcium chloride co-treated groups while no significant changes were observable in other treatment groups. Co-treatment with verapamil and NAC could completely reverse appraisal of these proteins phosphorylation upon exposure to ELF-EMF. These data highly suggests that ELF-EMF can induce necroptosis which can become aggravated by calcium overload.

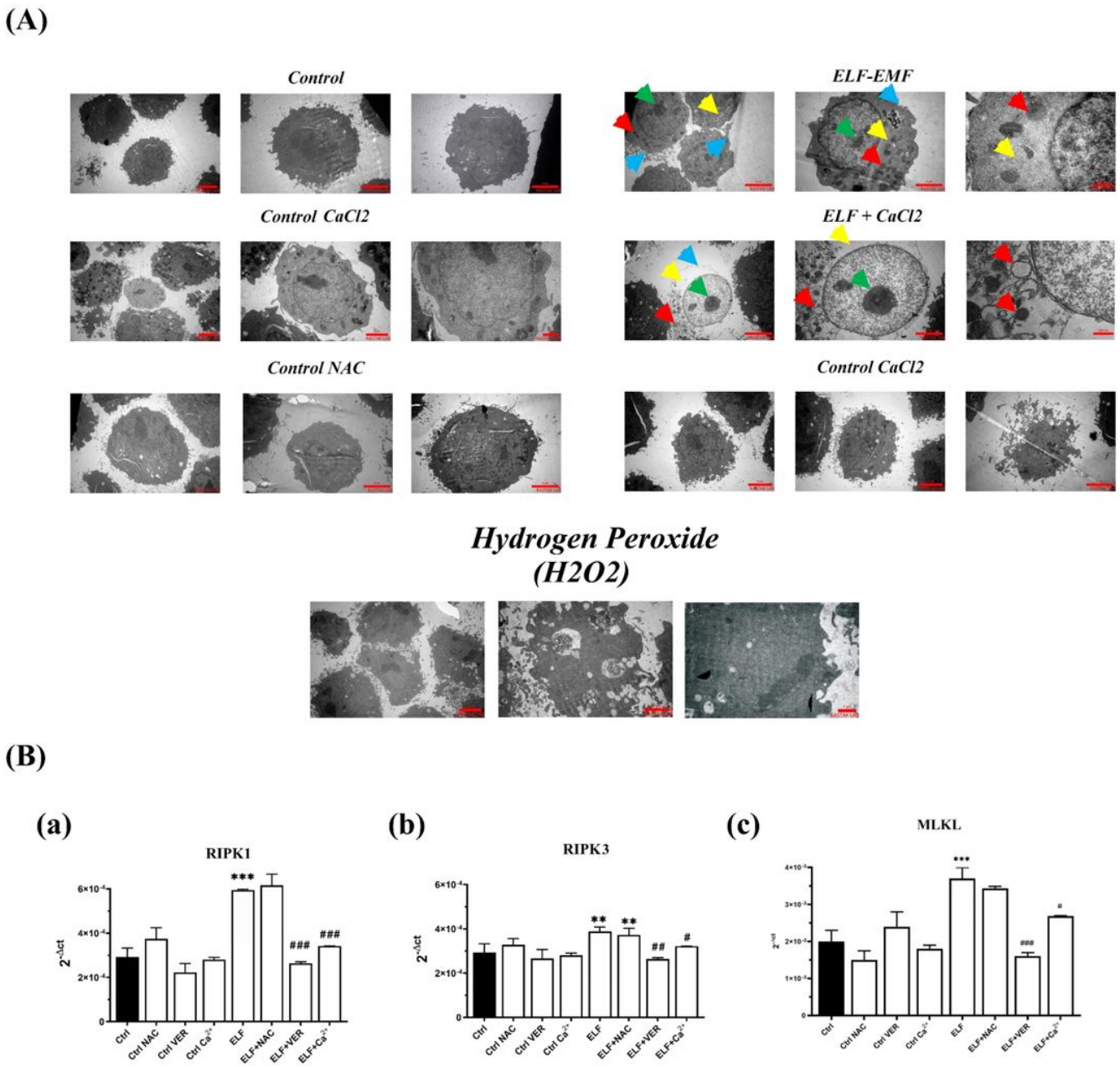

Figure 5

(A) TEM images obtained from normal MC4-L2 cells demonstrated well-preserved cytoplasmic organelles, as well as smoothly shaped nuclei encompassing heterochromatin shaped chromatin (fig. 5). Contrarily, H2O2 treated cells were used as apoptosis control group. This group of cells were mostly characterized by a marginated chromatin and formation of budding vesicles in the absence of swollen organelles. Upon examining ELF-EMF treated cells, in addition to the cells with typical apoptotic morphology, a large part of the cells demonstrated a translucent cytoplasm (yellow arrows), associated with disintegrated membrane (Blue arrow), organelle swelling (Red arrow) and condensed chromatin (Green arrow); all of which are typical characteristics of a necroptotic like cell death. The most prevalent form of morphological changes in other groups was either apoptotic form (NAC co-treated) or normal

form (NAC control, verapamil control and verapamil co-treated groups). (B) Consistent to the western blot analysis, evaluating mRNA expression of RIPK1/RIPK3/ and MLKL proteins by qPCR demonstrated a significantly increased expression in ELF-EMF and calcium chloride co-treated groups. Contrarily, expression of these factors were not significantly raised in groups receiving NAC and verapamil.

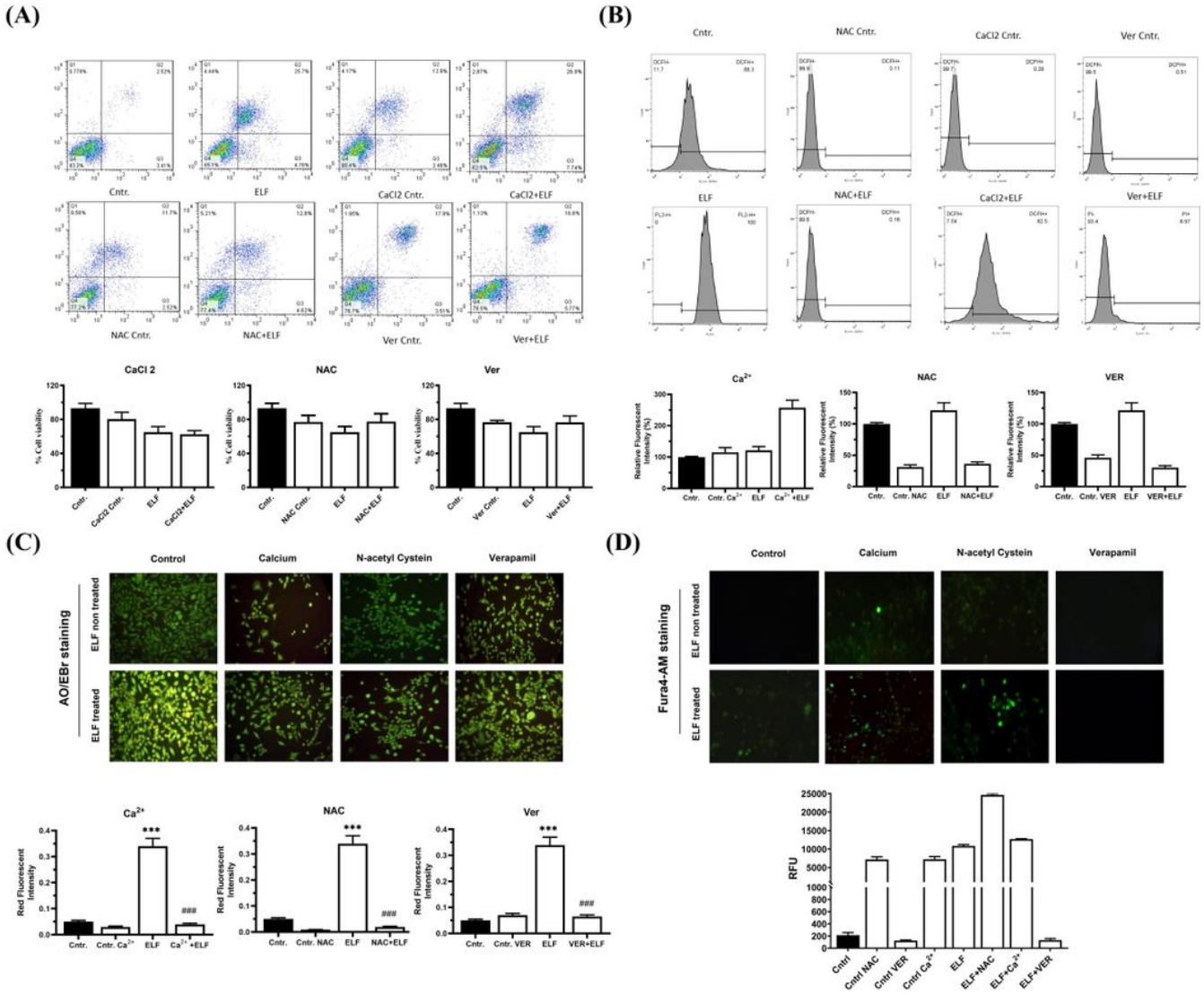

Figure 6

(A) ELF-EMF treatment could significantly increase double AV/ PI positive and AV positive PI negative subpopulation of cells which is indicative of induction of apoptosis, necroptosis or both. Very little increase in number of PI-/AV+ cells however, proposes the possibility of necroptotic cell death rather than apoptotic one. Co-treatment with NAC and verapamil could significantly reduce number of cell deaths while excess Ca2+ couldn't significantly enhance apoptotic response. (B) DCHF-DA staining demonstrating a significant increase in ROS levels following ELF-EMF exposure which was significantly attenuated upon co-treatment with NAC. Contrarily, calcium chloride co-treatment could effectively enhance intracellular overproduction of ROS. (C) Acridine orange staining demonstrated a significant

raise in formation of acidic vacuoles (red fluorescent), representative of autophagic response, upon exposure to ELF-EMF which could be significantly attenuated by co-treatment with NAC and verapamil. Calcium co-treatment didn’t have any significant effect on enhancement of autophagy. (D) Fluo-4 AM staining, demonstrating a significant raise in intracellular calcium concentration upon treatment with ELF-EMF. Co-treatment with NAC and calcium chloride could significantly enhance intracellular calcium overload while verapamil could effectively suppress intracellular calcium overload.